Characteristics and mixing enhancement of a self-throttling system in a supersonic flow with transverse injections

BIAN, Yifan, ZHAO, Majie, LI, Qinling <http://orcid.org/0000-0002-7191-9538> and YE, Taohong

Published version

BIAN, Yifan, ZHAO, Majie, LI, Qinling and YE, Taohong (2018). Characteristics and mixing enhancement of a self-throttling system in a supersonic flow with transverse injections. International Journal of Hydrogen Energy, 43 (29), 13550-13562.

Characteristics and Mixing Enhancement of a Self-throttling System in a Supersonic Flow with Transverse Injections

Yifan Bian[a], Majie Zhao[a], Qinling Li[b] & Taohong Ye[a,*]

[a] Department of Thermal Science and Energy Engineering, University of Science and Technology of China, Hefei, 230027, P.R. China

[b] Department of Engineering and Mathematics/MERI, Sheffield Hallam University, Sheffield, United Kingdom, S1 1WB

Abstract:

A three-dimensional self-throttling system is proposed in a scramjet combustor with transverse fuel jet, and investigated by Reynolds-averaged Navier-Stokes(RANS) simulations with the k-ω SST turbulence model. Numerical validation has been carried out against experiment and LES results. The effects of the jet-to-cross-flow momentum flux ratio and the throttling angle on mixing performance, fuel jet penetration depth and total pressure losses are all addressed. Through the proposed throttling system, the higher pressure upstream of the transverse fuel injection can drive part of the low momentum mainstream air into the downstream lower pressure region. The flow structures and the interactions between the shock waves and boundary layer are significantly modified to improve the mixing performance. The enhancement of mixing efficiency in the self-throttling system is closely related to the magnitude of the jet to crossflow momentum flux ratio, and a smaller throttling angle is found to further improve the mixing. On the other hand, the self-throttling system has a good performance in reducing the total pressure losses.

Keywords: Transverse injection, Self-throttling System, Supersonic flow, Mixing efficiency

1. Introduction

With increasing interest in supersonic and hypersonic flights, a good understanding of the mixing performance inside a scramjet combustor is essential. One of the critical issues is the mixing efficiency between fuel and air due to short residence time which is only about a millisecond under a typical flight condition [1]. Therefore, an effective fuel-air mixing strategy for the design of a scramjet combustor is required.

There are several methods for injecting fuel into a scramjet combustor, which are generally classified as two main categories [2], the wall injectors [3] and the strut injectors [4]. The wall injectors, i.e. transverse fuel injection through the wall of the combustor, has been widely used in the transverse jet in a supersonic crossflow (JISC) scramjet combustor [5].

Due to the complexity of JISC flow, the balance between better mixing performance and a

lower total pressure losses is found to be a challenge in high Mach number flows [6-7]. Many injection schemes have been proposed to improve the mixing and reduce the total pressure losses [8]. Multiple transverse injections, i.e. fuel-stage [9] or air-stage [10-11], has been proposed and studied by many researches. Pudsey & Boyce [12] suggested that the number of fuel injectors has a great influence on the mixing efficiency and penetration depth. And there is an optimal number of fuel jets required to maximize the mixing performance. For the best mixing efficiency, an optimal distance between the multiple injectors was suggested by Lee [9].

On the other hand, the boundary-layer separation upstream of injection causes a large flow separation, which leads to a distorted velocity profile and increases the total pressure losses. In order to control the interactions between the shock wave and the boundary layer, one effective way is to place throttling holes, i.e. the bleeding holes in Ref. [13], upstream the fuel jet where the shock wave strikes the boundary layer [14-15]. It is found by Chyu et al. [13] that flow separation induced by shock/boundary interactions can be eliminated by introducing throttling hole. These throttling holes can remove the low momentum portion of the boundary layer to decrease the boundary-layer thickness, which could increase the velocity at the near wall region and reduces the severity of boundary layer separation. This approach is used by Kodera et al. [16-17] to effectively intensify the combustion process in a scramjet combustor. Although, the boundary layer thickness and separation are in some way controlled, the mass flow through the throttling holes is not usually re-injected into the mainstream which leads to the loss of mainstream mass flow [18]. Obviously, there are several parameters related to the throttling efficiency, such as, the diameter, the geometry [19] and the angle of the throttling hole [13].

Between the upstream and downstream regions of the fuel injection, there exists a large pressure difference at wall which is roughly three times of the freestream pressure [20]. Hence, Han et al. [21] designed a new self-throttling system to avoid the total pressure losses and to increase the mixing efficiency. Two-dimensional numerical investigation of the self-throttling system shows that the fluid flow upstream from the higher-pressure region merges into the downstream lower pressure region, which can increase the fuel jet penetration and improve the mixing. However, the two-dimensional results of self-throttling system does not reflect the characteristics of a typical three-dimensional shock wave/boundary interactions and turbulent flow structure. Moreover, the geometrical parameters of the design of the self-throttling system are also deficient.

The main objectives of the current work are: (1) to propose a three-dimensional self-throttling system in a typical JISC combustor model; (2) to numerically investigate the mixing performance and total pressure losses with and without the self-throttling system. The paper is organized as follows. The physical model and numerical methods are introduced in Section 2, and the numerical and grid validation are also given in this section. Then results and detailed analysis

of three-dimensional self-throttling system in a typical JISC combustor model are exhibited in Section 3. Section 4 summarizes the conclusions of the paper.

2. Numerical Aspects and Validations

2.1 Governing Equations and Numerical Schemes

The governing equations of Reynolds-averaged Navier-Stokes(RANS) simulation for turbulent mixing flow are expressed as follows:

$$\frac{\partial \overline{\rho}}{\partial t} + \frac{\partial (\overline{\rho}\tilde{u}_i)}{\partial x_i} = 0 \tag{2.1}$$

$$\frac{\partial (\overline{\rho}\tilde{u}_i)}{\partial t} + \frac{\partial (\overline{\rho}\tilde{u}_i\tilde{u}_j)}{\partial x_j} = -\frac{\partial \overline{P}}{\partial x_i} + \frac{\partial}{\partial x_j}(\overline{\tau}_{ij} + \overline{\tau}_{ij}{}^{R}) \tag{2.2}$$

$$\frac{\partial (\overline{\rho}\tilde{H})}{\partial t} + \frac{\partial (\overline{\rho}\tilde{H}\tilde{u}_j)}{\partial x_j} = \frac{\partial \overline{\rho}}{\partial t} + \frac{\partial}{\partial x_j}\left(\frac{\mu_{eff}}{Pr_t}\frac{\partial \tilde{h}_s}{\partial x_j}\right) + \frac{\partial}{\partial x_j}\left[\tilde{u}_j(\overline{\tau}_{ij} + \overline{\tau}_{ij}{}^{R})\right] \tag{2.3}$$

$$\frac{\partial (\overline{\rho}\tilde{Y}_k)}{\partial t} + \frac{\partial (\overline{\rho}\tilde{Y}_k\tilde{u}_j)}{\partial x_j} = \frac{\partial}{\partial x_j}\left(\frac{\mu_{eff}}{Sc_t}\frac{\partial \tilde{Y}_k}{\partial x_j}\right) \tag{2.4}$$

where $\overline{\rho}$, $\tilde{u}$ and $\overline{P}$ are the density, velocity and pressure, respectively. $\tilde{h}_s$ is the sensible enthalpy, $\tilde{H}$ is the total enthalpy, where $\tilde{H} = \tilde{h}_s + \frac{1}{2}\tilde{u}_i{}^2$.The terms of $\overline{\tau}_{ij}$, $\overline{\tau}_{ij}{}^{R}$ are the molecule viscosity stress and Reynold stress. μ_{eff} is the effective viscosity, $\mu_{eff} = \mu + \mu_t$, where μ is the molecular viscosity computed by Sutherland's law $\mu = \frac{A_S\sqrt{T}}{1+\frac{T_S}{T}}$ and μ_t is the eddy viscosity closed by using the k-ω turbulence model in this study. $\tilde{Y}_k$ is the mass fraction. Turbulent Prandtl number Pr_t and Schmidt number Sc_t are assumed as 0.72. In this study, the Reynold stress $\overline{\tau}_{ij}{}^{R}$ is computed by k-ω SST turbulent model [22-23], which is a combination of the k-ω model in the near wall region and standard k-ε model away from the wall region. A switch function F_1 combines two turbulent models, which can be expressed as:

$$\frac{D\overline{\rho}k}{Dt} = \frac{\partial}{\partial x_j}\left[(\mu + \sigma_k\mu_t)\frac{\partial k}{\partial x_j}\right] + \overline{\tau}_{ij}{}^{R}\frac{\partial u_i}{\partial x_j} - \beta^*\overline{\rho}\omega k \tag{2.5}$$

$$\frac{D\overline{\rho}\omega}{Dt} = \frac{\partial}{\partial x_j}\left[(\mu + \sigma_\omega\mu_t)\frac{\partial \omega}{\partial x_j}\right] + \frac{\overline{\gamma}}{\nu_t}\overline{\tau}_{ij}{}^{R}\frac{\partial u_i}{\partial x_j} - \beta\overline{\rho}\omega^2 + 2\overline{\rho}(1-F_1)\sigma_{\omega 2}\frac{1}{\omega}\frac{\partial k}{\partial x_j}\frac{\partial \omega}{\partial x_j} \tag{2.6}$$

where $\nu_t = \frac{a_1 k}{\max(a_1\omega;|\Omega|F_2)}$ and $|\Omega|$ is the magnitude of vorticity. F_2 is a function to determine ν_t, and the values of parameters can be referred to Wilcox [24]. The k-ω SST model has been widely used to study supersonic transverse injection [25-28].

The thermodynamic state equation for ideal gas is expressed as:

$$\overline{P} = \overline{\rho}R\tilde{T} \tag{2.7}$$

where R is the mixture gas constant.

The above governing equations are solved by using a finite volume method based on the CFD software OpenFOAM [29]. The code is a density-based solver rhoCentralFoam[30] which

has been developed and validated in our previous simulations[31-33]. The convective fluxes are reconstructed using a second order TVD scheme and the second order central difference Gauss linear scheme is used for the viscous diffusion. Besides, the discretization of species transport equation implemented is the central upwind scheme. The inviscid solution is used as a predictor for the viscous solution.

2.2 Numerical Validations

The flow of a JISC, experimentally studied by Santiago & Dutton [34] and Everett et al. [35] and numerically investigated by many researches [36-38,31], is selected to validate the present numerical method. The inlet Mach number of the supersonic mainstream (cross-flow) is M_∞ = 1.6 while the jet Mach number is M_j = 1. The jet-to-cross-flow momentum flux ratio J, one of the most important parameters in terms of the mixing performance, is defined as:

$$J = \frac{(\overline{\rho}V^2)_j}{(\overline{\rho}V^2)_\infty} = \frac{(\gamma \overline{P} M^2)_j}{(\gamma \overline{P} M^2)_\infty} \tag{2.8}$$

where the subscript 'j' corresponds to the jet exit conditions and '∞' corresponds to the cross-flow inlet condition. γ is a constant specific-heats ratio, γ = 1.4. More details about the JISC flow parameters can be found in Table 1.

Table1 The JISC Flow Parameters in Santiago & Dutton [34] and Everett et al. [35]

Case0	Ma	Static Pressure (P/kPa)	Static Temperature (T/K)	Velocity (m/s)	Momentum flux ratio
Crossflow	1.6	56.7	198.48	437	J = 1.7
Fuel Jet	1	247	250.08	315	

The diameter of the jet orifice D is 4mm, located at 200mm downstream of the inlet and 320mm upstream of the exit. The width of the computational domain is from -48mm to 48mm and the height is 60mm (see Figure 1(a)). Three sets of mesh, i.e. coarse, medium and fine (mesh sizes from 251 × 71 × 81, 331 × 81 × 91, 371 × 91 × 101 in the X, Y, Z directions) with 1.54, 2.64 and 3.53 million grids, respectively, are generated. For all the three sets, mesh is refined near the jet orifice to capture the transverse injection flow characteristics and a "O" type mesh is adopted at the jet orifice to ensure the mesh quality (see Figure 1(b)). The first mesh height of boundary layer is 0.1mm to ensure the maximum value of y+ being less than 5, which has been proved a favorable mesh resolution for RANS simulations [27]. Simulations are run in parallel on the 48 cores of 2 Intel Xeon E5-2680 processors.

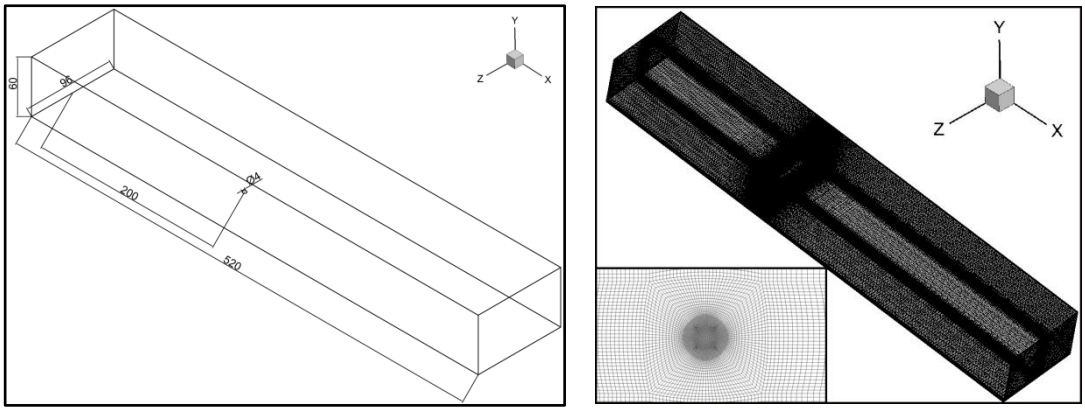

(a) Computational Domain (b) Computational Mesh

Figure 1 Computational Domain and Mesh

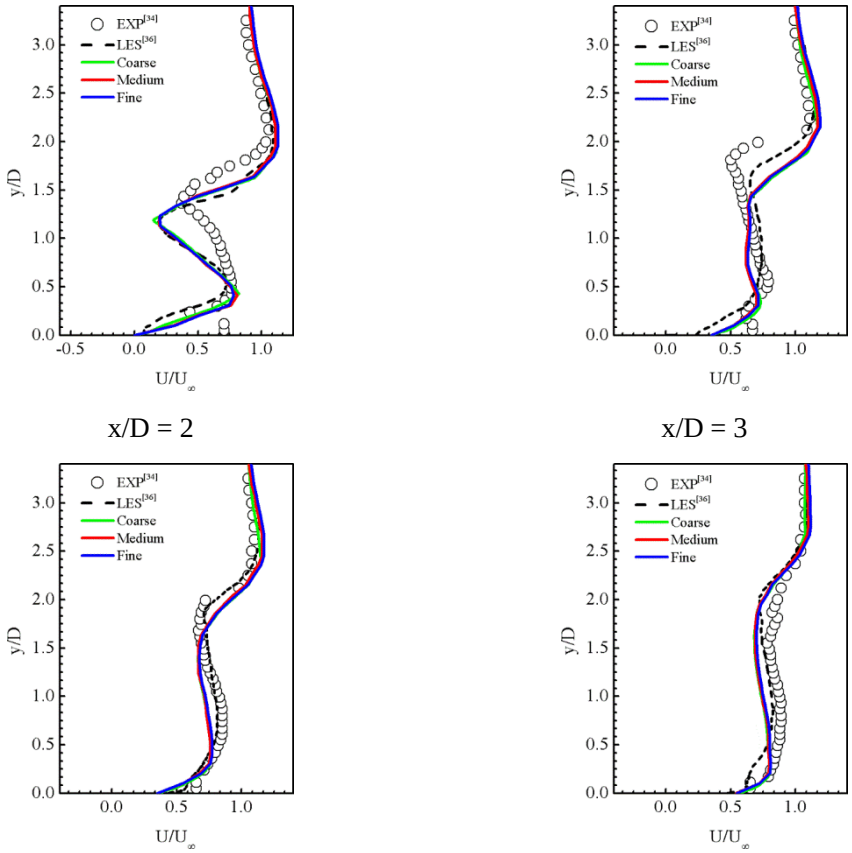

(a) Mean Streamwise Velocity U/U_∞ Distributions at x/D = 2, 3, 4 & 5 on the Symmetric Plane

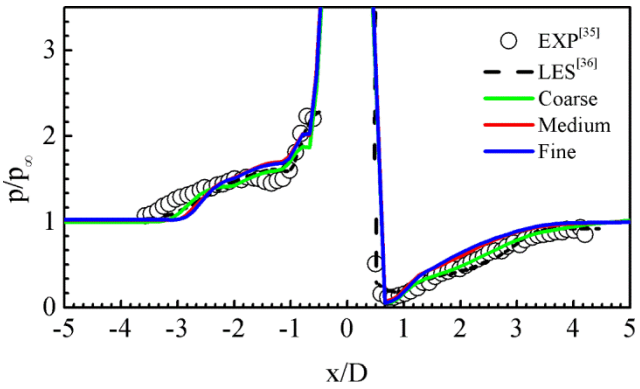

(b) Mean Wall-pressure p/p_∞ Distributions on the Symmetric Plane

Figure 2 Comparisons with Experiment [34-35] and LES [36] at Three Level Meshes: circle, experiment; dashed line, LES; solid line, RANS

Figure 2 shows the comparisons of the mean streamwise velocity U/U_∞ between experiment [34], LES [36] and the current predicted results with three levels of meshes at x/D = 2, 3, 4 and 5 on the symmetric plane (z/D = 0). The mean streamwise velocity with the k-ω SST turbulence model is in good agreement with that from LES, especially at x/D = 2 and 3 locations and both the current RANS and LES results are found to agree well with experiment, apart from y/D = 0.3-2 where the jet flow decays quickly, which is washed downstream. It is interesting to note that LES results fit experimental data very well at x/D = 4, and the current RANS results provide better agreement near the wall than the LES, especially at x/D = 5. Although there are some discrepancies between the numerical and experimental results, the wall-pressure trend is well captured by the present simulation(see Fig.2(b)). In general, the numerical approach can capture the characteristics of the flow fields in supersonic transverse injection accurately in the present study. This ensures the reliability of the following numerical investigation on the performance of the designed self-throttling system in a JISC combustor. It is also clearly shown that the mesh scale has only a slight difference to the numerical results. In order to ensure the grid independence for the more complex mixing flow with a self-throttling system, the grid scale of the medium mesh is adopted in the following RANS simulations.

3. Results and Discussion on the Self-throttling System

3.1 Description of the Self-throttling System and Simulations

The scramjet combustor with multiple transverse injection system on a typical flight condition, which is numerically studied by Lee [9], is referred as a benchmark in the present study. The inlet conditions are those of Mach 2 flight at 35km altitude in the standard atmosphere, where the static pressure and temperature are 146.6kPa and 1081K. The diameter of the hydrogen jet orifice D is 4mm, located at 200mm downstream of the inlet and 320mm upstream of the exit. The

static temperature of sonic hydrogen jet is 600K, and the magnitude of *J* is set to be one and two respectively.

Table2 Flow Parameters of the Supersonic Flow with Transverse Injection for All Cases

	Crossflow			Hydrogen Jet					Mesh Size
Cases	Ma_∞	P_∞(kPa)	T_∞(K)	Ma_j	P_j(kPa)	T_j(K)	*J*	θ	Cells
Case 1	2	146.6	1081	1	586.4	600	1	—	2640640
Case 2	2	146.6	1081	1	586.4	600	1	30°	3047005
Case 3	2	146.6	1081	1	586.4	600	1	60°	2898978
Case 4	2	146.6	1081	1	586.4	600	1	90°	2927102
Case 5	2	146.6	1081	1	1172.8	600	2	—	2640640
Case 6	2	146.6	1081	1	1172.8	600	2	30°	3047005
Case 7	2	146.6	1081	1	1172.8	600	2	60°	2898978
Case 8	2	146.6	1081	1	1172.8	600	2	90°	2927102

As for the self-throttling system, it takes the advantages of the boundary bleeding upstream the jet [19] and air-stage techniques [10]. The key parameters are the position, geometry, the number of throttling hole, the angle of throttling hole and the hydrogen jet-to-cross-flow momentum flux ratio *J*. Han et al. [21] proposed a 2D self-throttling system by using a channel to connect the upstream and downstream regions of the injection slot. In the present research, a three-dimensional self-throttling system is proposed for the benchmark combustor. Figure 3 shows the schematic geometry of the present JISC combustor with the self-throttling system, which has one shunting hole located at 8mm (x/D = 2) downstream of the hydrogen jet orifice, and three throttling holes located at 16mm, 32mm and 48mm upstream of the hydrogen jet orifice, respectively. Each of the above four orifices has the same diameter as the hydrogen injection orifice, and is located at the central symmetric plane. A channel with the length scale 72mm×8mm×8mm in the x-, y- and z-directions, is designed to connect the upstream and downstream orifice in the present study. In addition, the angle of the three throttling holes, θ (see Figure 3), one of the key parameter in boundary layer bleeding technique [13], is set to be 30°, 60° and 90°, respectively. The parameters of all the eight cases are listed in Table 2, in which the jet-to-cross-flow momentum flux ratio *J* =1 for Cases1-4 and *J* =2 for Case5-8, while the Case1 and Case5 are the baseline studies without the self-throttling. The computation domain is 520mm×96mm×60mm and the mesh size is basically the same as Case0 including mesh nodes are 331 × 81 × 91 nodes in the x-, y-, z-directions. The mesh count for all cases is listed in Table2 and the O-type block mesh is adopted at the orifice that is the same as Case0. As for the self-system domain, the first mesh height of boundary layer is 0.1mm to ensure the maximum value of y+ being less than 5 [9].

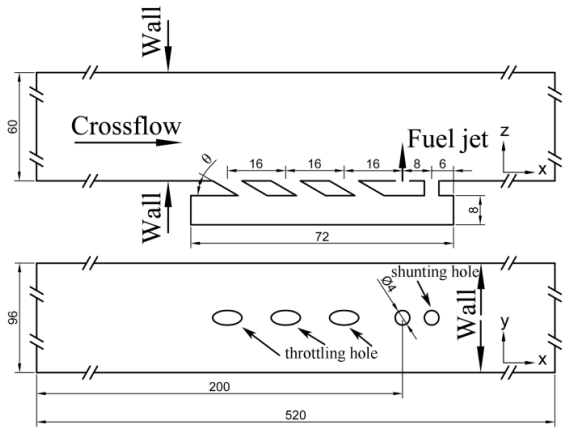

Figure 3 Schematic Geometry of the Benchmark JISC with the Self-throttling System

3.2 Effect of the Self-throttling System

To investigate the effects of the self-throttling system on JISC flow fields, the Mach number contours, the hydrogen mass fraction and the static pressure at the planes of x/D = 4, y/D = 0 and z/D = 0 of Case5 and Case6, respectively, are shown in Figure 4. Typical features of JISC flow field of Case5 without self-throttling system can be seen in Figure 4(a). The hydrogen jet expands through a Prandtl-Meyer fan at injection before the jet flow is compressed by the barrel shock and the Mach disk. Meanwhile, the fuel jet becomes an obstruction to the mainstream, resulting in a bow shock and a large flow separation region R1, this is because the interaction between the bow shock and boundary layer, while R4 is smaller due to the effects of throttling. A smaller recirculation zone R2 is present near the fields of the jet orifice due to effects of the barrel shock, and another one R3 in the wake of the transverse jet flow. On the plane x/D = 4, a pair of counter-rotating vortices (CVP), whose axis is in line with the crossflow direction, and a trailing counter-rotating vortex pair (TCVP) [39] are also clearly observed. When the self-throttling system is introduced, two significant features of Case6 could be observed in Figure 4(b). One is that there is no recirculation zone upstream of the barrel shock due to the upstream three throttling orifices which remove the low momentum portion of boundary layer. Besides, a shock generated by the upstream throttling hole [40] can decrease the freestream Mach number and weaken the interaction between the injection and freestream, leading to a lower adverse pressure gradient upstream the jet at z/D = 0 plane in Case6. It is also can be seen that separation region R4 is much smaller than R1. The other one is that the shunting air, from the higher-pressure region upstream of the hydrogen jet orifice to the lower pressure region downstream, lifts the hydrogen jet flow. This results in that the height of the center of Mach Disk rises from 1.4D in Case5 to 1.5D in Case6. Meanwhile, due to the shunting air, a bigger recirculation R5 exists in the wake of the shunting air flow, and that TCVP doesn't appear on x/D = 4 plane of Case6. It should be noted that TCVP can be observed downstream of the location x/D = 4, which is not shown in Figure 4. From

the hydrogen mass fraction contours at x/D = 4 plane, the mixing performance can be significantly improved by introducing the self-throttling system.

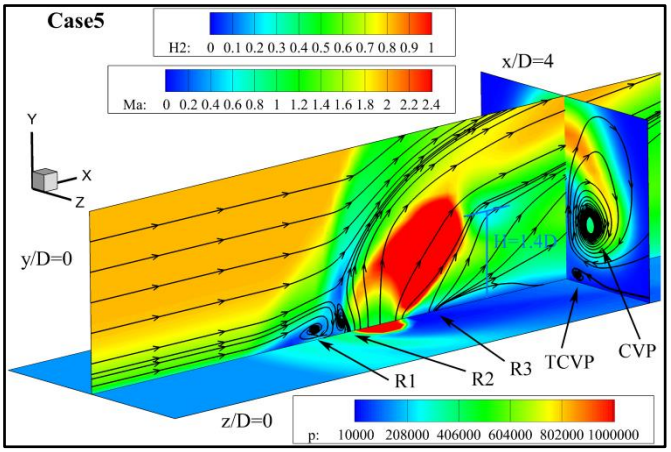

(a) Flow Features in JISC without the Self-throttling System

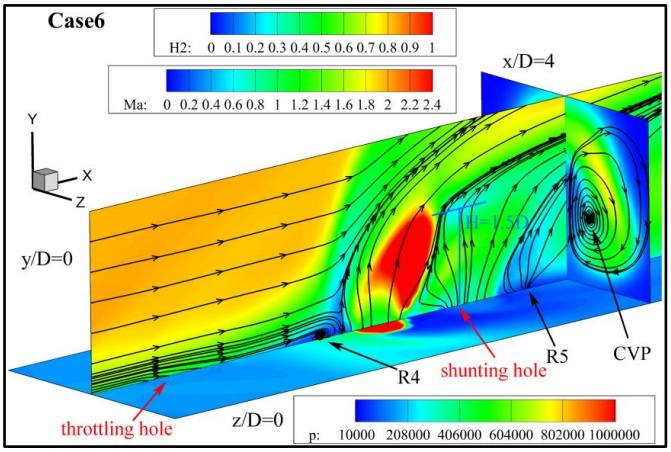

(b) Flow Features in JISC with the Self-throttling System

Figure 4 Typical Flow Features in JISC

The hydrogen mass fraction contours in the five cross section, x/D = 0, 2, 4, 6 & 8, and z/D=0 for Case1-2 and Case5-6 are shown in Figure 5. It is obvious that the CVP impacts the characteristic of the hydrogen mass fraction contour which presents a peach-shaped plume at the cross section x/D = 2 in Case1. With increasing downstream distance, the peach-shaped vortex transforms into kidney-shaped [41]. As for the Case2, the distribution of fuel mass fraction is significantly different from that in the Case1 especially at x/D = 2 and x/D = 4, where the hydrogen jet plume is changed by the shunting air, resulting in accelerating mixing from the maximum hydrogen mass fraction on the cross sections. Comparing Case1 with Case5, the case with a higher magnitude of *J* has a higher jet penetration into the crossflow and a larger proportion with higher mass fraction of hydrogen at different cross sections[38].

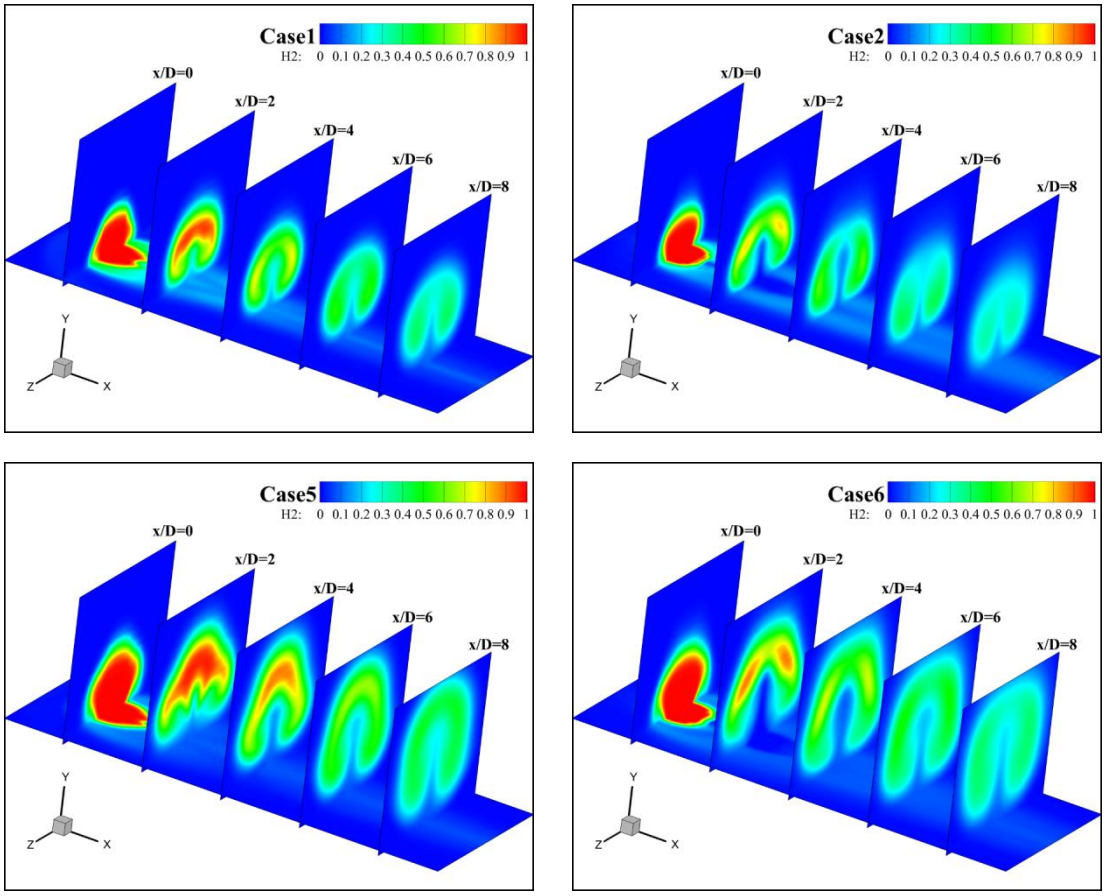

Figure 5 The Hydrogen Mass Fraction Contours at Five Cross Sections

The contours of the mean hydrogen mass fraction and the mean streamline of Case1, 2, 5 & 6 at the three cross sections, x/D = 1, 2 & 4 respectively, are shown in Figure 6. At the locations x/D = 1 and x/D = 2 of Case1 and Case5, one can see that the large-scale vortices CVP are generated by the interactions between the hydrogen jet and the crossflow [39]. Mainstream air can be entrained into the hydrogen plume under the influence of CVP which enhances the mixing. At the downstream locations x/D = 2 and x/D = 4, due to the suction effect of CVP on the wall, TCVP is generated below the CVP, which results in more air being entrained into the near wall region. TCVP and CVP play a key role in strengthening the mixing between the air and fuel. However, the shunting air destroys the TCVP structure by the self-throttling system at the location x/D = 2 of Case2 and Case6, leading to that the distribution of hydrogen mass fraction has changed dramatically. Although there is no TCVP in the region below CVP on the plane x/D = 2 of Case2 and Case6, the shunting air plays an alternative role to drive air directly into the hydrogen jet plume. With the development of CVP, TCVP appears again at the location of x/D = 4 in Case6.

Moreover, at the location x/D = 2 in Case5 and Case6, it can be seen that the shunting air changes the characteristics of the hydrogen mass fraction contour. Due to the process that accelerates the generation of CVP, the ambient air can be entrained into hydrogen early. Based on the above analysis of the impact by shunting air, the mixing between the air and fuel has a great

improvement in a short distance.

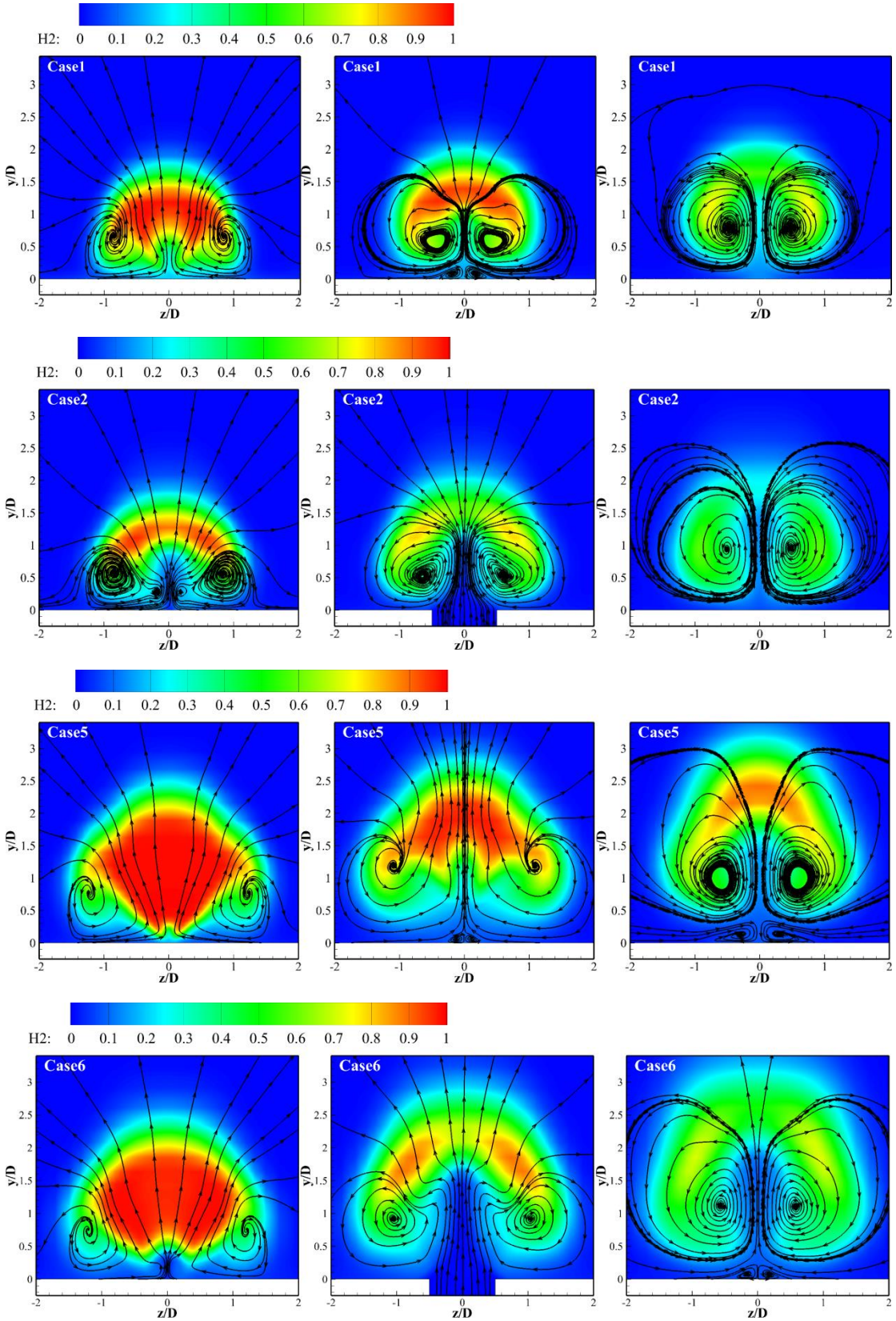

x/D = 1 x/D = 2 x/D = 4

Figure 6 The Hydrogen Mass Fraction Contours and Streamlines at Three Cross Sections

The role of the shunting air is similar to that of the air-stage system [10]. It is valuable to define a shunting air to cross-flow momentum flux ratio J_s to investigate the mixing process in the self-throttling system. In the present research, J_s is defined as follows:

$$J_s = \frac{(\overline{\rho}V^2)_s}{(\overline{\rho}V^2)_\infty} = \frac{(\gamma \overline{P} M^2)_s}{(\gamma \overline{P} M^2)_\infty} \tag{3.1}$$

where the subscript 's' corresponds to shunting air injection. Figure 7 shows the predicted J_s versus the throttling angle θ under two jet-to-cross-flow momentum flux ratios, J=1 and J=2. Generally, the case with the higher magnitude of J has the larger magnitude of J_s, and with increasing the throttling angle θ from 30° to 90° leads to lower J_s. Obviously, different throttling angles can lead to diverse outcomes and more detailed characteristics will be discussed next.

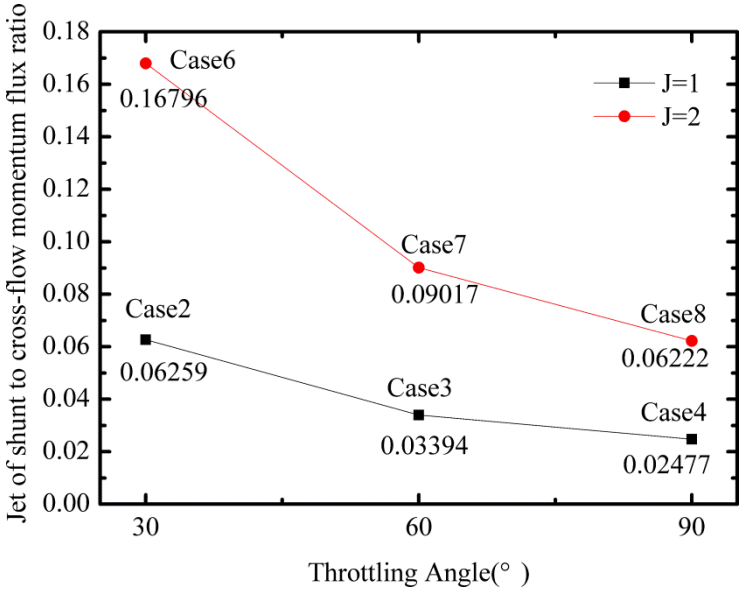

Figure 7 Shunting Air to Cross-flow Momentum Flux Ratio J_s Versus the Throttling Angle, θ

3.3 Fuel Jet Penetration Depth

The fuel jet penetration depth is one of the major parameters for wall heating flux and combustion efficiency of a JISC combustor [41], and is estimated with the center of mass of the hydrogen from the lower wall as follows [9],

$$P_{H_2}(x) = \iint \overline{\rho}\tilde{Y}_{H_2}\, y dy dz / \iint \overline{\rho}\tilde{Y}_{H_2}\, dy dz \tag{3.2}$$

where $\tilde{Y}_{H_2}$ is the mass fraction of hydrogen. Figure 8 shows the non-dimensional hydrogen jet penetration P_{H_2}/D versus x/D of all the studied eight cases listed in Table 2. It can be seen that the penetration depth increases by introducing the self-throttling system under the two jet to cross-flow momentum ratios J = 1 and J = 2, and also increases with decreasing the throttling angle θ. It can be seen in Figure 7 that Case2 and Case6 have the highest shunting air to cross-flow momentum flux ratio J_s under J = 1 and J = 2 respectively, however, Case4 and Case8 have the best preference of penetration depths, which indicates that penetration depth not only depends on the effect of shunting but also that of throttling. Furthermore, with increasing the

magnitude of *J*, the effect of the self-throttling system becomes evident. Comparing with Case1, the penetration depth of Case4 in a short distance (x/D = 10) increases by 22.15%. However, when the value of *J* is 2, the penetration depth of Case8 increases by 34.77% comparing with that of Case5. Besides, it is worth noting that the penetration depth slows down at the position of about x/D = 30, this is due to the influence of reflecting shock[31].

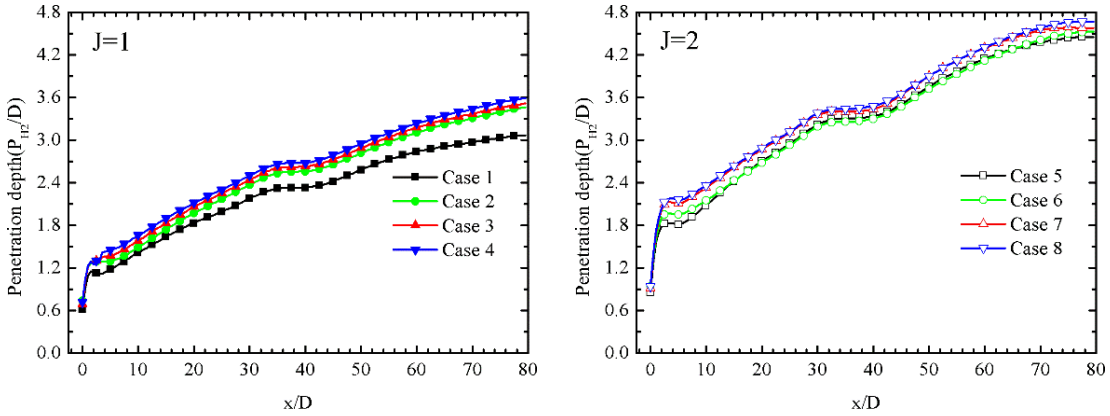

Figure 8 Comparison of the Penetration Depth

3.4 Mixing Efficiency

Figure 9 depicts the maximum hydrogen mass fraction $\tilde{Y}_{Max,H_2}$ on a cross-section plane, versus x/D. Obviously, $\tilde{Y}_{Max,H_2}$ is drastically reduced in the near field(x/D < 10) when the self-throttling system is introduced. The mixing process mainly depends on large-scale convection flow in the near field which is significantly influenced by the proposed self-throttling system. However, the curve of $\tilde{Y}_{Max,H_2}$ levels out with increasing downstream distance, where mixing process is dominated by the small-scale mass diffusion. Therefore, there is a transition from a convection-dominated regime to a diffusion-dominated regime [9]. When the self-throttling system is introduced, two factors can contribute to improve the mixing performance. Firstly, the shunting air enhances the large-scale vorticity and accelerates the flow mixing in the near field. Secondly, part of the air from upstream enters in the downstream region where hydrogen is rich to mix immediately [21]. With increasing downstream distance, the influence of the shunting air starts to decay as turbulent dissipation can weaken the strength of large scale convection. In addition, it can be seen that the Case2 and Case6, with the throttling angle of 30^o, have the fastest decay rate of $\tilde{Y}_{Max,H_2}$.

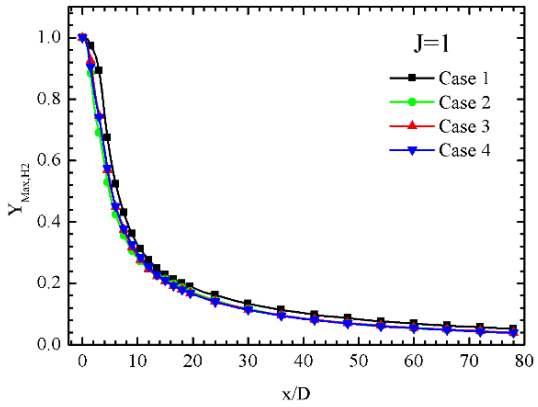

(a) Maximum Hydrogen Mass Fraction in All Fields (J = 1)

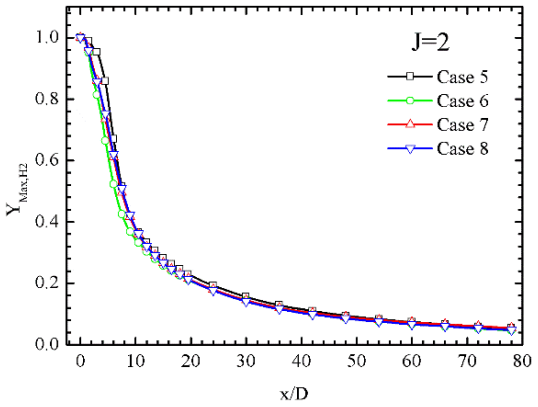

(b) Maximum Hydrogen Mass Fraction in All Fields (J = 2)

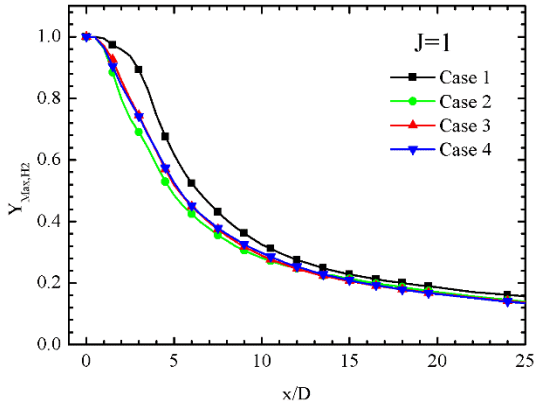

(c) Maximum Hydrogen Mass Fraction in the Near Fields of the Jet Orifice (J = 1)

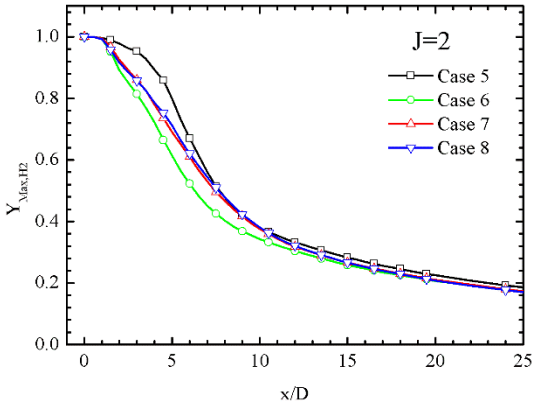

(d) Maximum Hydrogen Mass Fraction in the Near Fields of the Jet Orifice (J = 2)

Figure 9 Comparison of the Maximum Hydrogen Mass Fraction of All Cases

The mixing efficiency is defined as follows [43-45]:

$$\eta = \frac{\dot{m}_{hydrogen,mixed}}{\dot{m}_{hydrogen,total}} = \frac{\int \alpha_{react}\overline{\rho}\tilde{u}dA}{\int \alpha\overline{\rho}\tilde{u}dA} \tag{3.3}$$

where $\dot{m}_{hydrogen,mixed}$ is the mixed injectant hydrogen mass flow rate and $\dot{m}_{hydrogen,total}$ is the total injectant hydrogen flow rate, $\overline{\rho}$ and $\tilde{u}$ are the local density and velocity respectively. A is the cross-section area of the axial station where the mixing is evaluated. The α_{react} can be defined as follows:

$$\alpha_{react} = \begin{cases} \alpha, \alpha \leq \alpha_{stoic} \\ \frac{\alpha_{stoic}(1-\alpha)}{1-\alpha_{stoic}}, \alpha > \alpha_{stoic} \end{cases} \tag{3.4}$$

where α_{stoic} is stoichiometric mass fraction, and its value is 0.0291 for the hydrogen and air [46].

The mixing efficiency versus x/D for all the eight cases is plotted in Figure 10. At the initial stage of mixing especially before the position of x/D = 5, the mixing efficiency is mainly affected by convection, resulting in the rapid growth. With increasing the downstream distance, the diffusion has larger influence on mixing efficiency gradually. When the self-throttling system is introduced, the mixing efficiency has a large improvement within a short distance, which is

consistent with the results of Han, et al. [21]. One noticeable phenomenon is that the mixing efficiency has a biggest jump in Case 2 and Case 6 with the throttling angle of 30°, which is related to the maximum value of shunting air to cross-flow momentum flux ratio J_s.

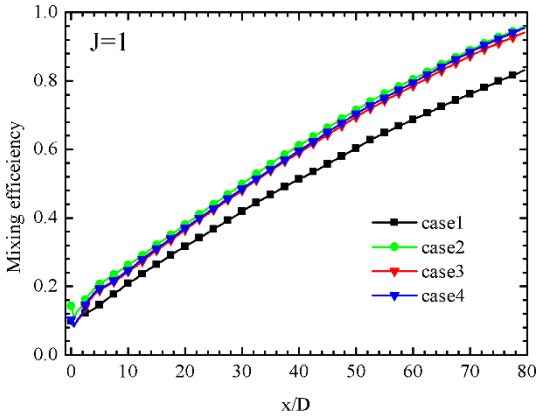

(a) Mixing Efficiency (J = 1)

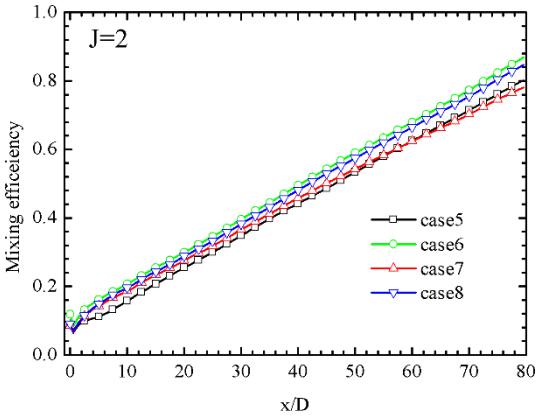

(b) Mixing Efficiency (J = 2)

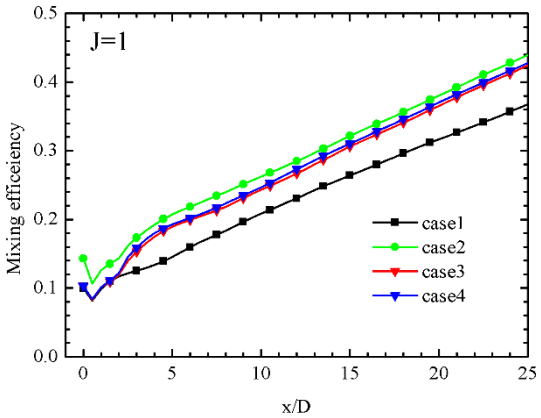

(c) Mixing Efficiency in the Near Fields of the Jet Orifice (J = 1)

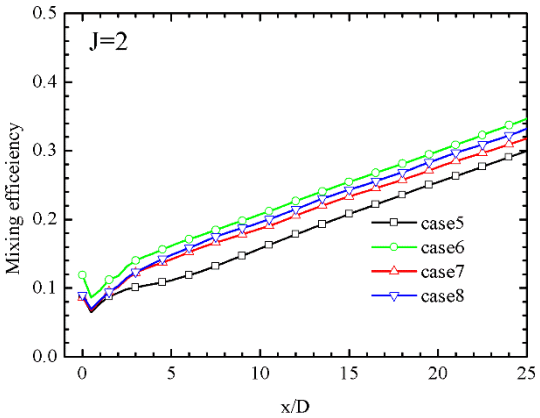

(d) Mixing Efficiency in the Near Fields of the Jet Orifice (J = 2)

Figure 10 Comparison of the Mixing Efficiencies Between All Cases

Further analysis of mixing efficiency at downstream location x/D = 5 is exhibited in Table 3 where η is the mixing efficiency. It shows that the case with smaller throttling angle 30° has the better mixing performance quantitatively. This means there is a strong relationship between mixing efficiency and throttling angle. Case2 and Case6 have the best mixing performance at the two jet-to-cross-flow momentum flux ratios due to the highest jet of shunt to cross-flow momentum flux ratio. Furthermore, with the increasing magnitude of J, the effect of self-throttling system on mixing is more significant.

Table 3 Mixing Efficiency at Plane x/D = 5

Case	J	η	$\Delta\eta = \frac{\eta - \eta_{case1}}{\eta_{case1}}$	Case	J	η	$\Delta\eta = \frac{\eta - \eta_{case5}}{\eta_{case5}}$
Case1	1	14.54%	—	Case5	2	11.13%	—
Case2	1	20.72%	42.50%	Case6	2	16.14%	45.01%
Case3	1	18.90%	29.99%	Case7	2	14.41%	29.47%

Case4	1	19.29%	32.67%	Case8	2	14.81%	33.06%

3.5 Total Pressure Losses

The shock waves caused by injection and the mixing process between the fuel and air are the two main aspects of total pressure losses. Therefore, it is worthwhile to investigate if there are additional losses of total pressure due to the mixing augmentation by the self-throttling system. The definition of average total pressure in the y-z plane is expressed in the following form [40]:

$$P_0(x) = \iint P_0 \overline{\rho}\tilde{u}dydz / \iint \overline{\rho}\tilde{u}dydz \tag{3.5}$$

where P_0 is the local total pressure. The profiles of the average total pressure, which is normalized by the inlet total pressure, along the streamwise direction are shown as Figure 11. In all cases, the total pressure decreases rapidly in the region before the injection but slowly at the position of injection. It can be shown obviously that self-throttling system has a good performance in reducing the total pressure losses. The reason is that the throttling holes upstream the hydrogen jet can remove the low momentum portion of the wall boundary layer, which has a control of the interaction between the boundary layer and the shock waves [13-15].

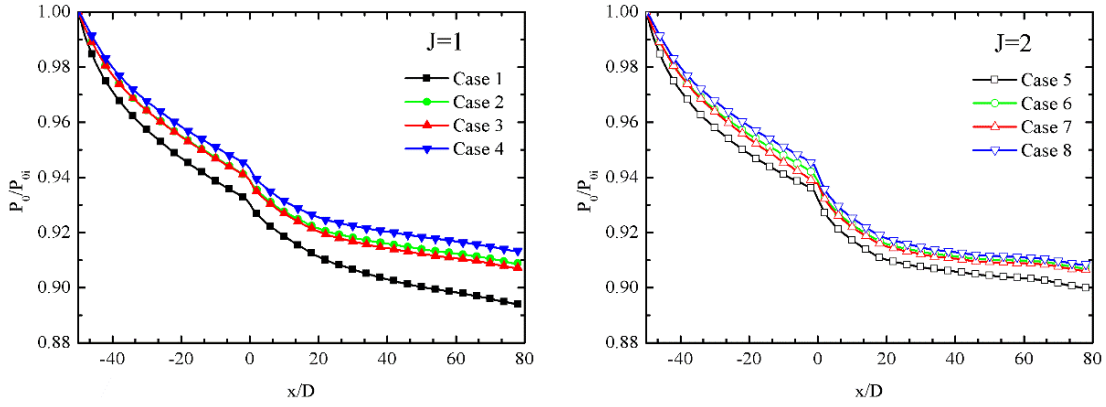

(a) (b)

Figure 11 The Normalized Averaged Total Pressure vs x/D

From Figure 11(a) and Figure 11(b), the total pressure losses in self-throttling system are strongly related to the magnitude of *J*. Generally, the cases with higher magnitude of *J* has less impact on the self-throttling system. Although, the throttling surface is the largest when the throttling angle is 30°, it is worth noting that 90° throttling angle has the best behavior in reducing the total pressure losses in the present study. The total pressure losses is influenced by various factors and needs further studies.

4. Conclusions

In the current study, the mixing characteristics of the self-throttling system in a scramjet combustor with transverse fuel injection are studied by RANS simulations with the k-ω SST turbulence model. The influence of two kinds of the parametric, the jet-to-cross-flow momentum

flux ratio *J* and the throttling angles, on mixing performance are conducted. The main conclusions can be drawn as follows:

(1) The fluid flow with high pressure upstream the injector can be partly shunted into downstream region by the proposed three-dimensional self-throttling system. The flow structures and the interactions between the shock waves and boundary layer are significantly modified to improve the mixing performance.

(2) The predicted results of the present studied cases show that small throttling angle leads to the higher shunting air to cross-flow momentum flux ratio and the better mixing performance. On the other hand, higher throttling angle performs better on the jet penetration and the total pressure losses due to the combined effects of the throttling and shunting.

(3) Based on the analysis of the characteristics of the jet penetration and mixing efficiency, the influence of the self-throttling system becomes significant under higher jet to cross-flow momentum flux ratio.

Further works should be carried out to investigate the effects of parameters such as geometry of throttling holes and the connecting channel on mixing and combustion.

Acknowledgement

This work is supported by the National Natural Science Foundation of China (Grant No. 91441117 and Grant No. 51576182). All numerical simulations have been performed on the supercomputing system, the Supercomputing Center in the University of Science and Technology of China.

Reference

[1] Kim J H, Yoon Y, Jeung I S, Huh H & Choi JY. Numerical study of mixing enhancement by shock waves in model scramjet engine[J]. AIAA journal, 2003, 41(6): 1074-1080.

[2] Gerlinger P, Stoll P, Kindler M, Schneider F & Aigner M. Numerical investigation of mixing and combustion enhancement in supersonic combustors by strut induced streamwise vorticity[J]. Aerospace Science and Technology, 2008, 12(2): 159-168.

[3] Cecere D, Ingenito A, Giacomazzi E, Romagnosi L & Bruno C. Hydrogen/air supersonic combustion for future hypersonic vehicles[J]. International Journal of Hydrogen Energy, 2011, 36(18): 11969-11984.

[4] Berglund M and Fureby C. LES of supersonic combustion in a scramjet engine model[J]. Proceedings of the Combustion Institute, 2007, 31(2): 2497-2504.

[5] Boyce R, Gerard S & Paull A. The HyShot scramjet flight experiment-flight data and CFD

calculations compared[M]//12th AIAA International Space Planes and Hypersonic Systems and Technologies. 2003: 7029.

[6] Sriram A T and Mathew J. Improved prediction of plane transverse jets in supersonic crossflows[J]. AIAA journal, 2006, 44(2): 405-408.

[7] Ukai T, Zare-Behtash H, Erdem E, Lo KH & Kontis K. Effectiveness of jet location on mixing characteristics inside a cavity in supersonic flow[J]. Experimental Thermal and Fluid Science, 2014, 52: 59-67.

[8] Constantine P G, Emory M & Larsson J. Exploiting active subspaces to quantify uncertainty in the numerical simulation of the HyShot II scramjet[J]. Journal of Computational Physics, 2015, 302: 1-20.

[9] Lee S H. Characteristics of dual transverse injection in scramjet combustor, Part 1: Mixing[J]. Journal of Propulsion and Power, 2006, 22(5): 1012-1019.

[10] Gerdroodbary M B, Amini Y, Ganji D D, et al. The flow feature of transverse hydrogen jet in presence of micro air jets in supersonic flow[J]. Advances in Space Research, 2017, 59(5): 1330-1340.

[11] Anazadehsayed A, Gerdroodbary M B, Amini Y, et al. Mixing augmentation of transverse hydrogen jet by injection of micro air jets in supersonic crossflow[J]. Acta Astronautica, 2017, 137: 403-414.

[12] Pudsey A S and Boyce R R. Numerical investigation of transverse jets through multiport injector arrays in a supersonic crossflow[J]. Journal of Propulsion and Power, 2010, 26(6): 1225-1236.

[13] Chyu W J, Rimlinger M J & Shih T I P. Control of shock-wave/boundary-layer interactions by bleed[J]. AIAA journal, 1995, 33(7): 1239-1247.

[14] Ghosh S, Choi J I & Edwards J R. Simulation of shock/boundary-layer interactions with bleed using immersed-boundary methods[J]. Journal of Propulsion and Power, 2010, 26(2): 203-214.

[15] Kouchi T, Mitani T & Masuya G. Numerical simulations in scramjet combustion with boundary-layer bleeding[J]. Journal of propulsion and power, 2005, 21(4): 642-649.

[16] Kodera M, Tomioka S, Kan K, Kanda T & Mitani T. Mach 6 Tests of Scramjet Engine with Boundary-Layer Bleeding and Two-Staged Injection[J]. Cancer Control Journal of the Moffitt Cancer Center, 2004, 22(9959):263-270.

[17] Kouchi T, Mitani T, Kodera M & Masuya G. Numerical experiments of scramjet combustion with boundary-layer bleeding[M]//12th AIAA International Space Planes and Hypersonic Systems and Technologies. 2003: 7038.

[18] Anderson B, Tinapple J & Surber L. Optimal control of shock wave turbulent boundary layer

interactions using micro-array actuation[C]//3rd AIAA Flow Control Conference. 2006: 3197.
[19] Syberg J and Koncsek J L. Bleed system design technology for supersonic inlets[J]. Journal of Aircraft, 1973, 10(7): 407-413.
[20] Spaid F W and Zukoski E E. A study of the interaction of gaseous jets from transverse slots with supersonic external flows[J]. AIAA journal, 1968, 6(2): 205-212.
[21] Han X, Ye T & Chen Y. Effects of self-throttling on combustion enhancement in supersonic flow with transverse injection[J]. International Journal of Hydrogen Energy, 2015, 40(25):8193-8205.
[22] Menter F R. Two-equation eddy-viscosity turbulence models for engineering applications[J]. AIAA journal, 1994, 32(8): 1598-1605.
[23] Menter F R, Kuntz M, Langtry R. Ten years of industrial experience with the SST turbulence model[J]. Turbulence, 2003.
[24] Wilcox D C. Turbulence modeling for CFD[M]. La Canada, CA: DCW industries, 1993.
[25] Gerdroodbary M B, Jahanian O, Mokhtari M. Influence of the angle of incident shock wave on mixing of transverse hydrogen micro-jets in supersonic crossflow[J]. International Journal of Hydrogen Energy, 2015, 40(30): 9590-9601.
[26] Gerdroodbary M B, Takami M R, Heidari H R, et al. Comparison of the single/multi transverse jets under the influence of shock wave in supersonic crossflow[J]. Acta Astronautica, 2016, 123: 283-291.
[27] Cai Z, Wang Z, Sun M & Bai XS. Effect of combustor geometry and fuel injection scheme on the combustion process in a supersonic flow[J]. Acta Astronautica, 2016, 129: 44-51.
[28] Shekarian A A, Tabejamaat S & Shoraka Y. Effects of incident shock wave on mixing and flame holding of hydrogen in supersonic air flow[J]. International Journal of Hydrogen Energy, 2014, 39(19): 10284-10292.
[29] Jasak H. Error Analysis and Estimation for the finite volume method with applications to fluid flows. Thesis submitted for the degree of doctor. Department of Mechanical Engineering, Imperial College of Science, 1996[J]. 1996.
[30] Greenshields C J, Weller H G, Gasparini L & Reese JM. Implementation of semi‐discrete, non‐staggered central schemes in a colocated, polyhedral, finite volume framework, for high‐speed viscous flows[J]. International journal for numerical methods in fluids, 2010, 63(1): 1-21.
[31] Zhao M, Ye T, Cao C, Zhou T & Zhu M. Study of sonic injection from circular injector into a supersonic cross-flow using large eddy simulation[J]. International Journal of Hydrogen Energy, 2016, 41(39): 17657-17669.
[32] Cao C, Ye T & Zhao M. Large eddy simulation of hydrogen/air scramjet combustion using tabulated thermo-chemistry approach[J]. Chinese Journal of Aeronautics, 2015, 28(5): 1316-1327.

[33] Zhao M, Zhou T, Ye T, Zhu M, & Zhang H. Large eddy simulation of reacting flow in a hydrogen jet into supersonic cross-flow combustor with an inlet compression ramp[J]. International Journal of Hydrogen Energy, 2017, 42(26): 16782-16792.

[34] Santiago J G and Dutton J C. Velocity measurements of a jet injected into a supersonic crossflow[J]. Journal of Propulsion and Power, 1997, 13(2): 264-273.

[35] Everett D E, Woodmansee M A, Dutton J C & Morris MJ. Wall Pressure Measurements for a Sonic Jet Injected Transversely into a Supersonic Crossflow[J]. Journal of Propulsion & Power, 2015, 14(6):861-868.

[36] Kawai S and Lele S K. Large-eddy simulation of jet mixing in supersonic crossflows[J]. AIAA journal, 2010, 48(9): 2063-2083.

[37] Chai X and Mahesh K. Simulations of high speed turbulent jets in crossflows[C]//49th AIAA Aerospace Sciences Meeting including the New Horizons Forum and Aerospace Exposition. 2010: 650.

[38] Wang G L, Chen L W & Lu X Y. Effects of the injector geometry on a sonic jet into a supersonic crossflow[J]. Science China Physics, Mechanics and Astronomy, 2013, 56(2): 366-377.

[39] Rana Z A, Thornber B & Drikakis D. Transverse jet injection into a supersonic turbulent cross-flow[J]. Physics of Fluids, 2011, 23(4): 046103.

[40] Yue L J, Lu H B, Xu X & Chang XY. Aerothermal characteristics of bleed slot in hypersonic flows[J]. SCIENCE CHINA Physics, Mechanics & Astronomy, 2015, 58(10): 104703.

[41] Li L, Huang W, Yan L & Li SB. Parametric effect on the mixing of the combination of a hydrogen porthole with an air porthole in transverse gaseous injection flow fields[J]. Acta Astronautica, 2017, 139: 435-448.

[42] Lee S H & Mitani T. Mixing augmentation of transverse injection in scramjet combustor[J]. Journal of Propulsion and Power, 2003, 19(1): 115-124.

[43] Segal C. The scramjet engine: processes and characteristics[M]. Cambridge University Press, 2009.

[44] Gruber M, Donbar J, Jackson T, Mathur T & Eklund D. Performance of an aerodynamic ramp fuel injector in a scramjet combustor[C]//36th AIAA/ASME/SAE/ASEE Joint Propulsion Conference and Exhibit. 2000: 3708.

[45] Gerdroodbary M B, Mokhtari M, Fallah K, et al. The influence of micro air jets on mixing augmentation of transverse hydrogen jet in supersonic flow[J]. International Journal of Hydrogen Energy, 2016, 41(47): 22497-22508.

[46] Huang W, Li L, Yan L & Liao L. Numerical exploration of mixing and combustion in a dual-mode combustor with backward-facing steps[J]. Acta Astronautica, 2016, 127: 572-578.